A full analytic potential energy curve for the $a\,^3\Sigma^+$ state of KLi from a limited vibrational data set

H. Salami, A. J. Ross, and P. Crozet
Laboratoire de Spectrométrie Ionique et Moléculaire, Université Lyon 1 and CNRS (Unité Mixte de Recherche 5579), 43 Boulevard du 11 Novembre 1918, F-69622 Villeurbanne, France

W. Jastrzebski
Institute of Physics, Polish Academy of Sciences, Al. Lotników 32/46, 02668 Warsaw, Poland

P. Kowalczyk
Institute of Experimental Physics, Warsaw University, ul. Hoża 69, 00681 Warsaw, Poland

R. J. Le Roy
Department of Chemistry, University of Waterloo, Waterloo, Ontario N2L 3G1, Canada

(Received 2 February 2007; accepted 3 April 2007; published online 18 May 2007)

Fourier transform spectra of near-infrared laser-induced fluorescence in $^{39}K^6Li$ show transitions to high vibrational levels of both the $X\,^1\Sigma^+$ and $a\,^3\Sigma^+$ electronic states. These include 147 transitions into six vibrational levels of the $a\,^3\Sigma^+$ state, which lie between 7 and 88 cm^{-1} below the dissociation asymptote. Unfortunately, their energies span less than 30% of the well depth. However, fitting those data to eigenvalues of analytical model potential functions whose outer limbs incorporate the theoretically predicted long-range form, $V(R) \simeq \mathcal{D} - C_6/R^6 - C_8/R^8$, yields complete, plausible potential curves for this state. The best fits converge to remarkably similar solutions which indicate that $\mathcal{D}_e = 287(\pm 4)$ cm^{-1} and $R_e = 4.99(\pm 0.09)$ Å for the $a\,^3\Sigma^+$ state of KLi, with $\omega_e = 47.3(\pm 1.4)$ and $44.2(\pm 1.5)$ cm^{-1} for $^{39}K^6Li$ and $^{39}K^7Li$, respectively. Properties of the resulting potential are similar to those of a published *ab initio* potential and are consistent with those of the analogous states of Li_2, K_2, Na_2, and NaK. © *2007 American Institute of Physics*. [DOI: 10.1063/1.2734973]

I. INTRODUCTION

The objective of the present work was to determine an experimental potential energy curve for the $a\,^3\Sigma^+$ state of KLi, which correlates with ground-state $K(4s)+Li(2s)$ atoms. This effort was motivated by recent developments in cold-atom photoassociation of heteronuclear species such as NaCs,[1] LiCs,[2] RbCs, and KRb.[3] The much lighter KLi molecule is likely to be difficult to see in cold-atom photoassociation, not only because of the obvious problem of preparing high densities of the constituent atoms in a single trap but also because of its relatively small C_6 coefficient, which leads to poor Franck-Condon probabilities for photoassociation into bound states, as noted by Wang and Stwalley.[4] Nevertheless, it offers an interesting situation in which all boson-plus-fermion pair combinations occur for the atoms forming a single species, and since collisions between heteronuclear atoms result in preferential formation of molecules in triplet rather than singlet states, the lowest triplet state is of particular importance. The condensation of a potassium-lithium mixture under ultracold conditions is currently being investigated at Innsbruck, in an extension of their studies of crossover between Bose-Einstein condensates and Bardeen-Cooper-Schrieffer superfluid phases in lithium[5] to mixtures of heteronuclear fermionic quantum gases.

Earlier experimental work has characterized several singlet states of this molecule. However, the only observations of triplet states were some isolated perturbations involving levels located approximately 18 400 cm^{-1} above the minimum of the electronic ground state of K^7Li, which have been identified using polarization labeling spectroscopy[6] as either $b\,^3\Pi \sim B\,^1\Pi$ or $c\,^3\Sigma^+ \sim B\,^1\Pi$ interactions. The present work reports observations of high vibrational levels of the $a\,^3\Sigma^+$ triplet state of the $^{39}K^6Li$ isotopologue. As for the analogous states of the homonuclear alkali dimers, the attractive dispersion contributions to the interatomic potential only outweigh repulsive exchange contributions at large internuclear distance, so this state is expected to be weakly bound. An *ab initio* calculation by Rousseau *et al.*[7] predicts $\mathcal{D}_e = 273$ cm^{-1} for the $a\,^3\Sigma^+$ state of KLi. In the absence of any observations of the lowest vibrational levels, the conventional method of constructing a potential energy curve, performing a Rydberg-Klein-Rees calculation[8] based on conventional molecular constants, is impractical. The present analysis is therefore based on performing a direct fit of the experimental data to an analytical potential function which is based on a modified form of the Morse potential, but whose outer limb takes on the inverse-power form predicted by theory,[9,10]

$$V(R) \simeq \mathcal{D} - \frac{C_6}{R^6} - \frac{C_8}{R^8} - \cdots , \tag{1}$$

in which the energy at the potential asymptote, $\mathcal{D} = 6216.31(\pm 0.07)$ cm^{-1} relative to the ground-state potential minimum, is known from our recent (unpublished) experimental work on the $X\,^1\Sigma^+$ state,[11] and the C_n coefficients are known from theory. The present work uses $C_6 = 1.119$

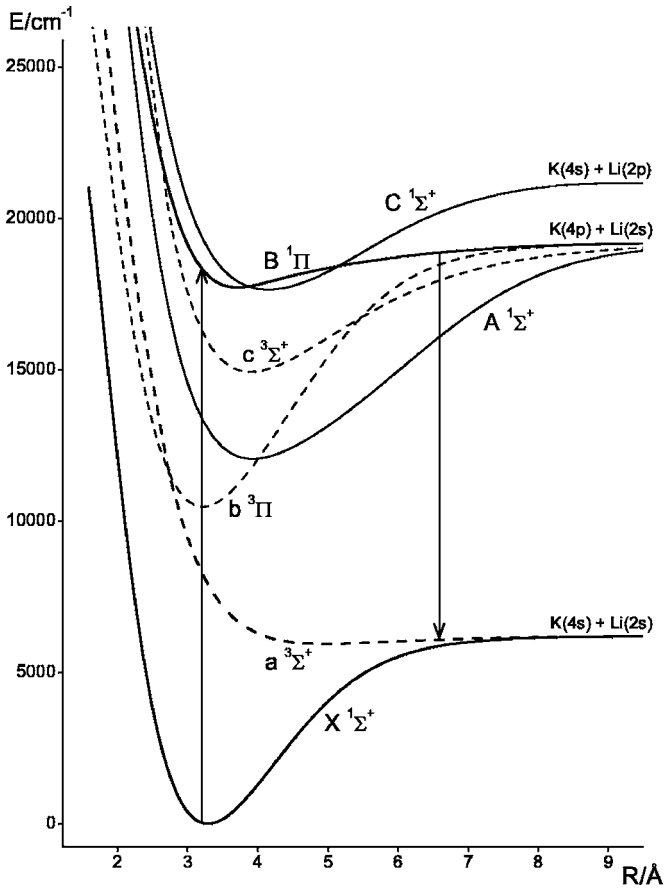

FIG. 1. *Ab initio* potential energy curves for low-lying electronic states of KLi (Ref. 7) are used to illustrate possible mechanisms for reaching the triplet states.

$\times 10^7$ cm^{-1} Å^6 from Ref. 12 and $C_8=2.63\times 10^8$ cm^{-1} Å^8 from Ref. 13.

II. EXPERIMENT

KLi molecules were formed in the central section of a linear, dual-temperature heat pipe.[14] The central zone, initially loaded with a 1 g sample of lithium metal, was maintained at 590 °C. Roughly 2 g of potassium metal were placed in the outer segments of the heat pipe, which were then heated to 300 °C. The heat pipe was operated with (typically) 5 mbars of Ar buffer gas. Vapor outside the central part of the heat pipe contains very little Li. Fluorescence was excited with emission from an Ar$^+$-pumped ring dye laser (SP 380D), collected using a pierced mirror, and analyzed on a Fourier transform interferometer (Bomem DA3), with appropriate optical filters in place to reduce laser scatter from the heat pipe windows. The instrumental resolution was usually ~0.05 cm^{-1}. The detector was either a Si avalanche ($\lambda<950$ nm) or an InGaAs ($900<\lambda<1600$ nm) photodiode.

We first tried to excite mixed $A\ ^1\Sigma^+/b\ ^3\Pi$ levels by operating the dye laser around 900 nm, since spin-orbit mixing of the triplet and singlet states correlating at long range with $M(s)+M(p)$ atoms has often provided a gateway to the triplet manifolds of the alkali dimers. The attempt was unsuccessful because the laser beam was completely absorbed by

TABLE I. List of resonances giving access to triplet fluorescence in $^{39}K^6Li$. Laser wave numbers are wavemeter readings.

$\bar{\nu}_{\text{laser}}$ (cm^{-1})	*B-X* pump	$T_{v,J}$	$v''(a\ ^3\Sigma^+)$[a]
18 263.57	*R*(16) 10-1	18 678.771	5–8
18 243.35	*P*(18) 10-1	18 678.771	5–8
18 368.55	*Q*(12) 16-2	18 970.504	5–8
18 347.24	*Q*(22) 17-2	19 049.444	5–8
18 454.72	*Q*(33) 17-1	19 114.212	5
18 316.21	*P*(25) 17-2	19 059.568	5
18 315.73	*Q*(29) 18-2	19 121.698	5, 6
18 334.59	*Q*(30) 19-2	19 157.592	6
18 316.99	*P*(31) 19-2	19 157.632	6
18 303.02	*R*(11) 20-3	19 115.523	7–9
18 303.02	*P*(10) 20-3	19 109.281	7–9
18 306.95	*R*(10) 20-3	19 113.173	7–10
18 310.61	*R*(9) 20-3	19 111.158	7–9
18 310.61	*P*(8) 20-3	19 106.057	7, 8
18 313.87	*R*(8) 20-3	19 109.282	7–9
18 313.87	*P*(7) 20-3	19 104.717	7, 8
18 316.71	*R*(7) 20-3	19 107.582	7–9
18 316.71	*P*(6) 20-3	19 103.569	7, 8
18 300.72	*Q*(11) 20-3	19 113.251	7–10
18 312.18	*Q*(8) 20-3	19 107.591	7, 8
18 315.18	*Q*(7) 20-3	19 106.065	7–9
18 462.72	*Q*(23) 22-2	19 178.131	7–9

[a]Assuming $v_{\min}=5$, see text.

K_2 vapor formed in the cooler region of the heat pipe, and no intensity remained to excite the KLi, which was present only in the central section.

We next looked for singlet/triplet mixed levels in the upper vibrational levels of the $B\ ^1\Pi$ state, accessed with Coumarin 6 dye. Polarization labeling spectra recorded in Warsaw had identified one such level in $^{39}K^7Li$, $B\ ^1\Pi\ v'=22$, $J'=39f$, but only singlet fluorescence series (from quite different pump transitions, both in KLi and in impurity NaK) were recorded when the laser was tuned to excite it. A tedious but fairly systematic investigation was therefore undertaken to observe the triplets. Figure 1 indicates that by exciting KLi approximately 150 cm^{-1} below the $B\ ^1\Pi$ state dissociation limit of $Li(2s)+K(4p\ ^2P_{3/2})$, triplet fluorescence should occur in the region of 11 000–12 500 cm^{-1}. The dye laser was tuned until fluorescence signals were detected through narrowband optical filters centered at 850±50 nm. Fluorescence from promising excitation lines was then recorded over a wider range (11 000–15 000 cm^{-1}) at a resolution of 0.05 cm^{-1} on the Fourier transform (FT) spectrometer. In many instances, the IR signal revealed transitions to the high vibrational levels of the singlet ground-state $X\ ^1\Sigma^+$, plus the potassium *D* lines, but some triplet transitions were

TABLE II. Band constants (in cm^{-1}) for levels of the ground $X\ ^1\Sigma^+$ state of $^{39}K^6Li$ involved in this work (Ref. 11).

v	G_v	B_v	$10^6 D_v$
0	112.820	0.292 506	1.984
1	336.413	0.290 162	1.978
2	557.101	0.287 795	2.000
3	774.864	0.285 373	2.010

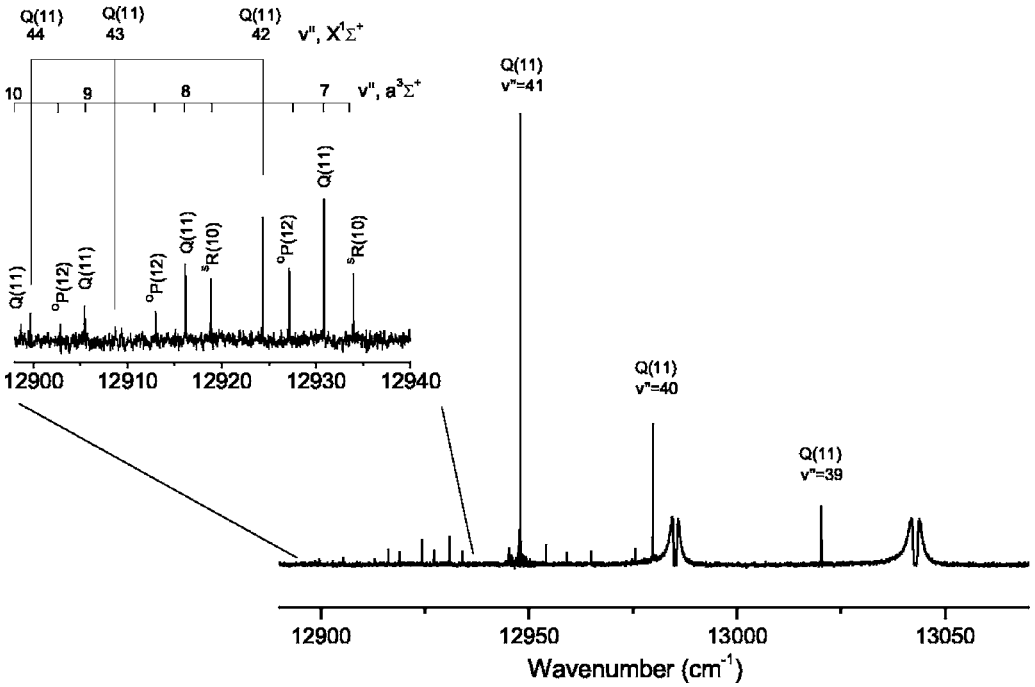

FIG. 2. Fluorescence from $v'=20$, $J'=11f$ of $B\,^1\Pi$, with Q lines seen in the $B-X$ system, and Q lines with strong ^SR, ^OP satellites to $a\,^3\Sigma^+$. The potassium D lines at 12 985.17 and 13 042.88 cm^{-1} are self-absorbed.

identified both in direct fluorescence and in a collisionally induced system. Analysis revealed that this triplet emission was always from the minor isotopologue $^{39}K^6Li$. The experiments were therefore repeated using a sample of enriched ^6Li (Euriso-Top) and high purity (99.99%) K in order to enhance the KLi signal and eliminate the (strong and frequently observed) fluorescence signals from NaK impurity. The list of resonances accessing levels of mixed singlet/triplet character is given in Table I; the upper-state energies are referenced to the minimum of the ground-state potential curve. Constants for the X-state levels involved in the excitation transitions are listed in Table II.[11]

The spectra provide a fairly complete set of measurements for the $X\,^1\Sigma^+$ ground state; they enabled us to locate its potential minimum and use it as an energy origin for the fluorescence emission into both states. It also allowed us to use a near-dissociation theory analysis[15,16] of the ground-state vibrational energies to establish a dissociation energy of $\mathcal{D}_e=6216.31(\pm0.07)$ cm^{-1} for the X state of the lighter isotopologue, $^{39}K^6Li$. This value is believed to be more reliable than the estimate for $^{39}K^7Li$ quoted by Martin *et al.*,[17] since the present observations extend closer to the dissociation limit. A full description of work on the ground state is outside the scope of this paper and will be presented as part of a full combined-isotopologue analysis of the ground-state data for both $^{39}K^6Li$ and $^{39}K^7Li$.[11]

Many of the triplet fluorescence series recorded were from levels $5\leqslant J\leqslant 12$ of $v'=20$ in the $B\,^1\Pi$ state. They gave fluorescence to high vibrational levels of both $X\,^1\Sigma^+$ and $a\,^3\Sigma^+$. As expected from Franck-Condon factors, emission from $v'=20$ in the $B\,^1\Pi$ state included strong transitions near 770 nm to $v''=38-40$ of $X\,^1\Sigma^+$. Very close to these bands, we also observed some patterns of both P/R doublets and ^OP, Q, ^SR triplets, but with different vibrational spacings. An example of such a spectrum is presented in Fig. 2, and the corresponding energy level pattern is drawn to scale in Fig. 3. Upper-state combination differences established that emission to $X\,^1\Sigma^+$ and $a\,^3\Sigma^+$ comes from common upper levels. The observation of strong Q branches in the triplet system suggests that the perturbing upper-state lending triplet character is a high vibrational level of $b\,^3\Pi$ (with $v'>50$). Once the lower-state assignments from $v'=20$ were secure, the fragmentary observations from other levels were readily identified.

A collisionally-induced triplet system consisting of P and R branches was observed only when the laser pumped $v'=10$, $J'=17e$ of the $B\,^1\Pi$ state. This spectrum is illustrated in Fig. 4. Upper-state combination differences taken within the rotational relaxation patterns did not match those of the very strong singlet system, so it was more difficult to establish an absolute energy scale for the electronic states involved. The upper trace in Fig. 4 shows a small (0.085 cm^{-1}) line/extra-line splitting in the $P(18)$ line, which is also visible in $R(16)$, but nowhere else. The lower wave number component corresponds to a transition from the triplet component, and the higher one comes from the dominantly singlet level of the $B\,^1\Pi$ state lying at $T'=18\,678.855$ cm^{-1}, from which fluorescence is also observed back to the $X\,^1\Sigma^+$ state. All transitions seen as rotational relaxation come from a single vibrational level of the triplet state (presumed to be high v' in $c\,^3\Sigma^+$), and fluorescence occurs to four vibrational levels of the $a\,^3\Sigma^+$ state.

The 8.4–23.8 cm^{-1} vibrational spacings measured in the triplet state are much smaller than the ω_e value of 44 cm^{-1} predicted *ab initio*.[7] This implies that we do not observe the lowest levels of the $a\,^3\Sigma^+$ state. Our direct emission measurements locate the observed levels with respect to the elec-

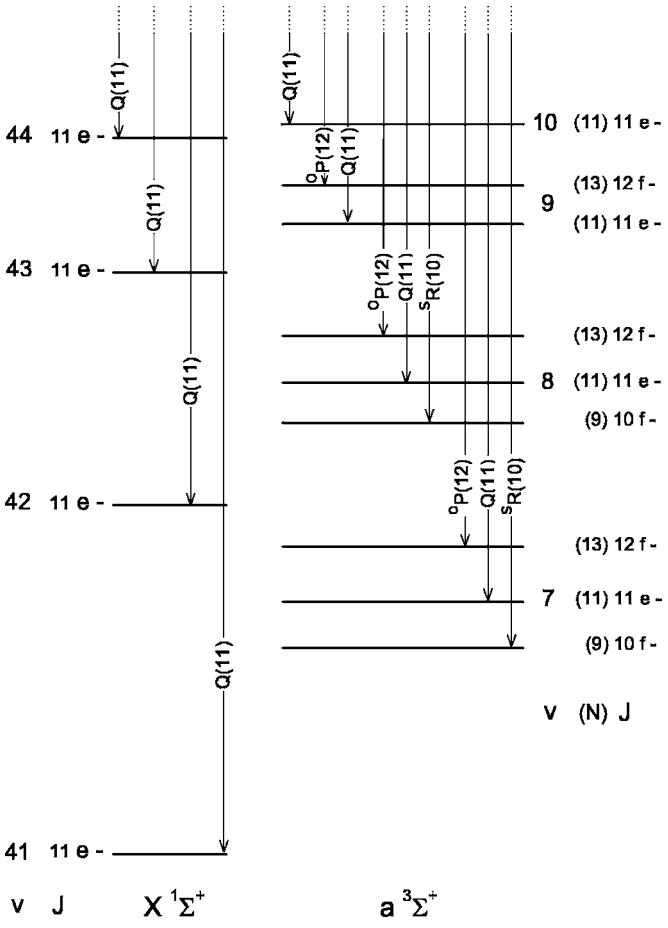

FIG. 3. High lying vibrational levels of $X\,^1\Sigma^+$ and $a\,^3\Sigma^+$ observed in fluorescence from $v'=20$, $J'=11f$ in the $B\,^1\Pi$ state, drawn to scale.

tronic ground state, and hence also with respect to the $a\,^3\Sigma^+$ state asymptote, and indicate that the lowest observed a-state vibrational level has a binding energy of 87.5 cm^{-1}. In the absence of equivalent observations for other isotopologues, the data themselves do not provide a definitive vibrational assignment. However, based on the *ab initio* potential, the most reasonable hypothesis was that the lowest observed vibrational level would be $v_{min}=5(\pm1)$. This assignment is confirmed by the analysis reported below.

III. PRELIMINARY ANALYSIS

A total of 147 transitions into six vibrational levels of the $a\,^3\Sigma^+$ state of $^{39}K^6Li$ were observed; a listing of these data is available as supplementary material.[18] No spin-rotation structure was resolved in the spectra, and levels were initially represented by band parameters,

$$T_{v,N}=T_v+B_v[N(N+1)]-D_v[N(N+1)]^2+H_v[N(N+1)]^3+L_v[N(N+1)]^4. \quad (2)$$

The upper-state energies for the direct fluorescence (relative to the ground-state potential minimum) are given in Table I. The rotational levels in the (unassigned) vibrational level of $c\,^3\Sigma^+$ were also represented by Eq. (2). The parameters determined for the $a\,^3\Sigma^+$ state, given in Table III, allow the observed transitions to be recalculated with an unweighted root-mean-square error of 0.006 cm^{-1}, which is close to the estimated experimental uncertainty of 0.005 cm^{-1}. Because the potential well for the $a\,^3\Sigma^+$ state is so shallow, contributions from high-order distortion constants are significant. Trial values for H_v and L_v were initially calculated from the *ab initio* curve, but in the final "parameter fit" summarized by Table III, the fixed distortion constants (values with no uncertainties) were calculated from the optimized potential curve reported below.

Direct fits to Dunham representations of the energy levels were successful only when the low-order terms were constrained, and the associated choice of Y_{10}, Y_{01},…, etc., was quite arbitrary. Without such constraints, fits of different orders yielded very different, and often implausible, extrapolations to $v=0$. Attempts to fit the energy levels and rotational constants to near-dissociation expansion (NDE) models[15,19,20] were also unsuccessful, in that the extrapolation to $v=0$ was very model dependent, even though the energy of the asymptote $\mathcal{D}$ is known from work on the X state (analysis of $B\rightarrow X$ transitions recorded in the same set of spectra), and the long-range potential coefficients C_6 and C_8 are known from theory.[12,13] The analogous NDE rotational fits extrapolated particularly poorly, leading to physically implausible shapes in the low-v extrapolation region.

IV. DIRECT-POTENTIAL-FIT ANALYSIS

A. Methodology

In the absence of any experimental observations of low vibrational levels of the $a\,^3\Sigma^+$ state, constructing a reliable potential energy curve was something of a challenge. Fitting the data to a numerical "spline-pointwise" potential[21,22] yielded a function whose eigenvalues reproduced the observed energies to ±0.02 cm^{-1} (approximately four times the estimated experimental uncertainty). However, the resulting curve had an unrealistic broad, flat minimum, and there was no obvious way of correcting that behavior other than by *ad hoc* manual adjustment of individual potential function points.

Since the $a\,^3\Sigma^+$ state correlates with two S-state atoms, the attractive outer branch of its potential is due to a sum of attractive inverse-power terms, with the powers of the two leading terms being $n=6$ and $m=8$. Moreover, reliable estimates of the leading dispersion coefficients C_6 and C_8 are available from theory.[12,13] We therefore chose to fit the data to an analytical potential function based on the structure of a "modified Morse potential,"[23] which was designed to incorporate the theoretically predicted long-range behavior of Eq. (1). This "Morse/long-range" (MLR) potential has the general form[9,10]

$$V_{MLR}(R)=\mathcal{D}_e\left\{1-\frac{u_{LR}(R)}{u_{LR}(R_e)}e^{-\phi_{MLR}(R)y_p(R)}\right\}^2, \quad (3)$$

in which $\mathcal{D}_e$ is the well depth and R_e is the equilibrium internuclear distance. The desired long-range behavior is defined by

$$u_{LR}(R)=\frac{C_n}{R^n}+\frac{C_m}{R^m}, \quad (4)$$

where $u_{LR}(R_e)$ is the value of this function at R_e, and

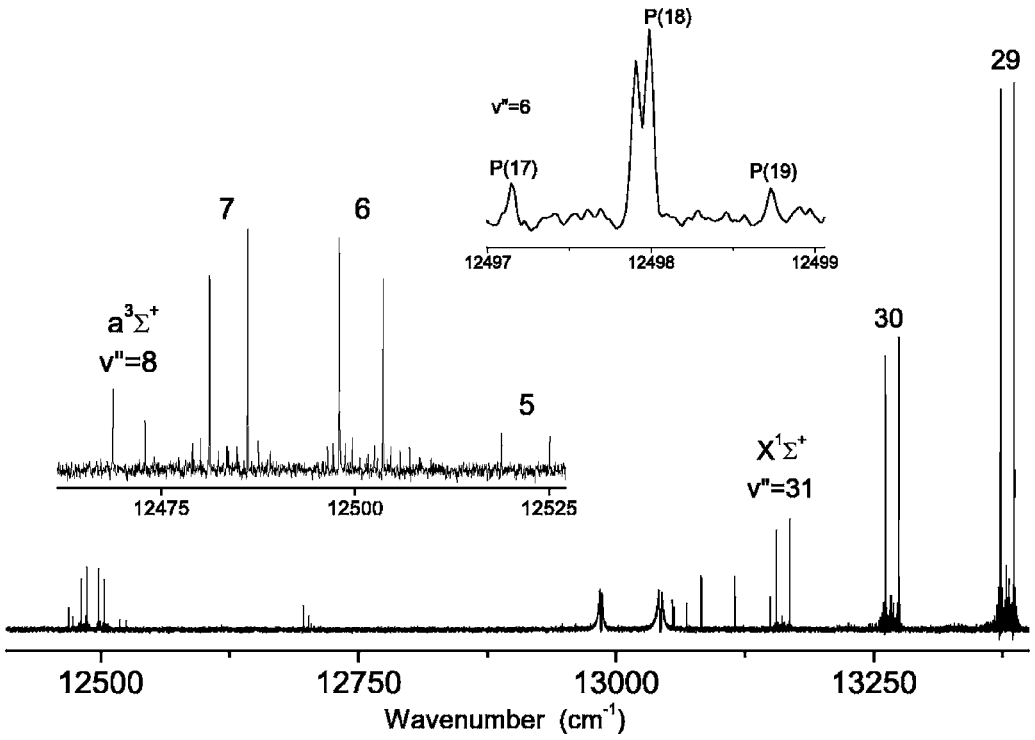

FIG. 4. FT emission spectrum showing well-separated transitions to the $a\,^3\Sigma^+$ and $X\,^1\Sigma^+$ states of K^6Li obtained following excitation to $B\,^1\Pi$ ($v'=10$, $J'=17$, e parity). Rotational relaxation patterns are seen in both the singlet and triplet systems; they originate from different upper states.

$$y_p(R) \equiv (R^p - R_e^p)/(R^p + R_e^p) \tag{5}$$

is a dimensionless radial expansion variable. This function implicitly incorporates the two leading inverse power terms in the long-range potential of Eq. (1), since at long range it takes on the form

$$V(R) \simeq \mathcal{D}_e - u_{\mathrm{LR}}(R) = \mathcal{D}_e - \frac{C_n}{R^n} - \frac{C_m}{R^m}. \tag{6}$$

The power p in the definition of $y_p(R)$ is typically a small positive integer (say, $p=3-5$) chosen to minimize the possibility of irregular potential function behavior at long range, outside the region over which the data are sensitive to it.[24–26] However, if the potential is to achieve the long-range behavior of Eq. (6), necessarily $p>(m-n)$ (here, $p>2$).[10] The exponent coefficient in Eq. (3) is a polynomial in $y_p(R)$ which is constrained to asymptotically approach a specified limiting value of

$$\phi_\infty = \ln\{2\mathcal{D}_e/u_{\mathrm{LR}}(R_e)\} = \ln\{2\mathcal{D}_e/[C_n/(R_e)^n + C_m/(R_e)^m]\} \tag{7}$$

and is expressed in the form

$$\phi_{\mathrm{MLR}}(R) = [1 - y_p(R)]\sum_{i=0}^{N_S} \phi_i y_p(R)^i + y_p(R)\phi_\infty \quad \text{for } R \leqslant R_e, \tag{8}$$

$$\phi_{\mathrm{MLR}}(R) = [1 - y_p(R)]\sum_{i=0}^{N_L} \phi_i y_p(R)^i + y_p(R)\phi_\infty \quad \text{for } R > R_e. \tag{9}$$

While there is only a single set of ϕ_i coefficients, the polynomial orders N_S and N_L may be chosen to be either the same or different for $R \leqslant R_e$ and $R > R_e$. If $N_S \neq N_L$, derivatives of the potential of order $\geqslant(\min\{N_S, N_L\}+3)$ would have small discontinuities at the one point $R=R_e$. While this situation would not be ideal, it has been found that setting $N_S < N_L$ is

TABLE III. Band constant parameters (in cm^{-1}) for the observed levels of $a\,^3\Sigma^+$ state $^{39}K^6Li$. Numbers in parentheses are uncertainties in the last digits shown; parameters with no uncertainties were held fixed at calculated values (see text).

	$v=v_{\min}$	$v_{\min}+1$	$v_{\min}+2$	$v_{\min}+3$	$v_{\min}+4$	$v_{\min}+5$
G_v	6128.868(9)	6152.672(8)	6172.512(3)	6188.497(3)	6200.639(12)	6208.987(19)
10^2B_v	9.297(6)	8.456(5)	7.630(4)	6.675(5)	5.605(21)	4.521(14)
10^6D_v	6.296(116)	6.192(102)	8.615(152)	9.783(220)	12.18(84)	19.36
10^9H_v	−0.84(6)	−2.09(6)	−2.09(16)	−4.79(27)	−5.59	−13.23
$10^{12}L_v$	−0.20	−0.36	−0.70	−1.62	−4.73	−18.83

sometimes necessary to prevent the resulting potential function from having unphysical inflection or turnover behavior in the short-range extrapolation region.[24–26] In any case, even if $\min\{N_S, N_L\}$ is fairly small, this would be a very modest shortcoming. The MLR potential function model is discussed in more detail in Ref. 10.

Our fits using this model potential were performed using program DPOTFIT,[27] which performs direct fits of experimental transition energies to level energy difference calculated from the assumed parametrized potential energy function(s). The upper-state term energies for the direct fluorescence originating from the B-state levels listed in Table I were constrained to values established from $B \rightarrow X$ emission and the X-state analysis. In effect, the a-state lower levels of these transitions were defined as binding energies relative to the common a- and X-state asymptote. In contrast, transitions associated with the collisionally induced triplet system were treated as fluorescence series originating in the seven distinct upper-state $T'_{v',J}$ levels, and those series-origin energies were also determined in the fit.

B. Results

In contrast to our (unsatisfactory) attempt to fit the data using the numerical spline-pointwise potential form, the fact that the potential well for this state is entirely due to attractive inverse-power van der Waals dispersion energy terms means that the MLR potential form provides a strong stabilizing constraint on the analysis. Using three possible assignments for the lowest of the six observed vibrational levels, $v_{\min}=4$, 5, and 6, fits were performed to a range of models characterized by different values of the expansion variable parameter p and of the exponent polynomial orders N_S and N_L. In all of these fits, the long-range potential coefficients were held fixed at the values given by theory:[12,13] $C_6 = 1.119 \times 10^7$ cm^{-1} Å^6 and $C_8 = 2.63 \times 10^8$ cm^{-1} Å^8. As expected with this type of model,[9,10] all else being equal, the number of parameters required to achieve a given quality of fit increases with the value of p. For all three vibrational assignments, good fits were achieved for a variety of distinct models.

Figure 5 presents plots of potential curves associated with the three choices of $v_{\min}$; all were obtained from fits with dimensionless standard errors $\lesssim 1$ (i.e., unweighted standard deviations of $\lesssim 0.005$ cm^{-1}). The most noteworthy feature of these results is the close similarity of the different curves for a given value of $v_{\min}$. This shows that in spite of their limited vibrational range, the data have strong predictive ability regarding the unobserved lower vibrational levels. This reflects the fact that the substantial degree of centrifugal distortion affecting the spacings between the observed levels effectively defines high moments of the potential and of $1/R^2$, which only allow a limited degree of variance in the nature of the potential function in the low-energy extrapolation region. As would be expected, the dispersion among the different possible potential minimum positions associated with a given vibrational assignment increases as the distance from the lowest observed level to the minimum increases with $v_{\min}$.

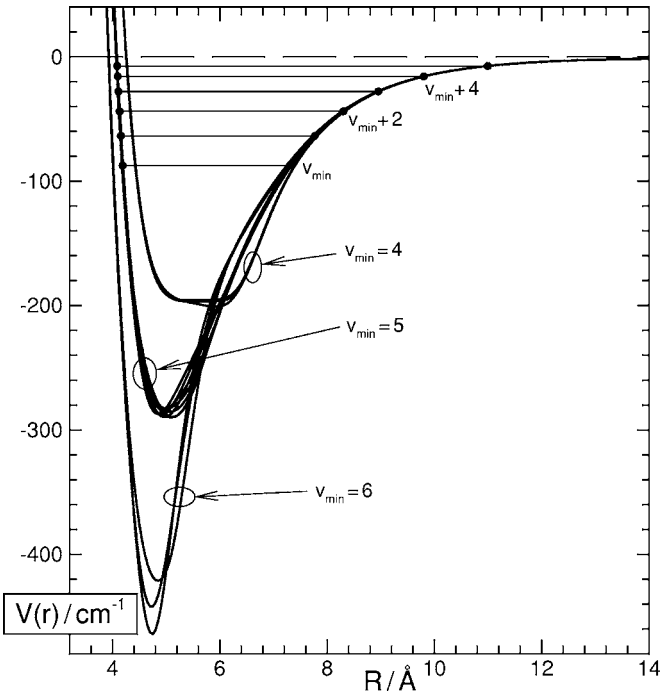

FIG. 5. Four fitted potentials for $v_{\min}=4$, eight for $v_{\min}=5$, and three for $v_{\min}=6$, all of which account for all of the available data within the estimated experimental uncertainties (standard errors $\lesssim 0.005$ cm^{-1}).

The implausible square-bottom shapes of the four curves in Fig. 5 associated with the choice $v_{\min}=4$ provide a clear indication that this vibrational assignment would be incorrect. Unfortunately, the shapes of the potential for $v_{\min}=5$ and 6 do not provide any clear discrimination of this sort, and the correct vibrational assignment cannot be determined from the data alone. However, comparisons with theory and with results for similar chemical systems do resolve this ambiguity.

The *ab initio* well depth of $\mathcal{D}_e = 273$ cm^{-1} reported by Rousseau *et al.*[7] is unlikely to be in error by more than 10%–20%. Inspection of Fig. 5 therefore indicates that the correct vibrational assignment must be $v_{\min}=5$. As an independent check on this conclusion, Table IV lists the experimental $\mathcal{D}_e$ and R_e values for the $a\ ^3\Sigma^+$ states of Li_2, Na_2, K_2, NaK, and of KLi (the latter assuming our $v_{\min}=5$ assignment), and compares the values for the heteronuclear species both with *ab initio* results and with values obtained by applying standard combining rules to the experimental values for the associated homonuclear species.[28] The close agreement of our $v_{\min}=5$ results with the combining-rule values clearly confirms the validity of our assignment, while the level of agreement found for NaK attests to the validity of this approach. The rest of the analysis reported below is therefore based on this vibrational assignment.

Of course, the standard error of a fit is not the only criterion by which a given fitted potential energy curve should be judged. Some models with $p=4$ for which the dimensionless root-mean-square deviation $\overline{dd}$ was only slightly greater than 1.0 were eliminated for being physically implausible, because their outer branches had three inflection points in the extrapolation region below the lowest observed vibrational level. Less obvious irregularities in some of these

TABLE IV. Well depths $\mathcal{D}_e$ and equilibrium internuclear distances R_e for the $a\,^3\Sigma^+_{(ii)}$ states of Li_2, Na_2, K_2, NaK, and KLi. Use of an arithmetic mean for R_e and of a harmonic mean $[\epsilon_{ij}=2\epsilon_{ii}\epsilon_{jj}/(\epsilon_{ii}+\epsilon_{jj})]$ for $\mathcal{D}_e$ is based on experience for rare-gas van der Waals interactions (Ref. 28).

		$^7Li_2$	$^{23}Na_2$	$^{39}K_2$	$^{23}Na\,^{39}K$	$^{39}K\,^7Li$
R_e (Å)	Experiment	4.173[a]	5.166[b]	5.773[c]	5.462[d]	4.99(±0.09)
	Ab initio				5.45[e]	4.974[f]
	Arithmetic mean combining rule				5.469	4.973
$\mathcal{D}_e$ (cm^{-1})	Experiment	333.69[a]	173.65[b]	252.74[g]	207.86[d]	287.0(±4)
	Ab initio				197[e]	273[f]
	Harmonic mean combining rule				205.9	287.6

[a]From Ref. 29.
[b]From Ref. 37.
[c]From Ref. 38.
[d]From Ref. 31.
[e]From Ref. 39.
[f]From Ref. 7.
[g]From Ref. 30.

"good-fit" solutions were revealed when vibrational spacings and rotational and distortion constants were calculated from the potentials. For the analogous states of Li_2,[29] K_2,[30] NaK,[31] KRb,[32] and NaRb,[33,34] values of $\Delta G_{v+1/2}$ and B_v smoothly decrease and D_v smoothly increases as v increases, so in addition to requiring a potential to have only one inflection point, we also required these three properties to vary smoothly and monotonically with v.

Our final objective was to obtain both an optimum potential function model and realistic estimates of the overall uncertainties in its well depth and equilibrium distance. The eight $v_{\min}=5$ potentials shown in Fig. 5 all yield good fits to the data, have physically reasonable shapes, and have appropriate monotonically varying spectroscopic constants. We have no *a priori* reason for preferring one particular model, and hence conclude that the best estimates of the well depth and equilibrium distance which can be obtained at this time are the averages of the parameter values for those eight cases: $\mathcal{D}_e=287(\pm4)$ cm^{-1} and $R_e=4.99(\pm0.09)$ Å. Our estimated uncertainties in these quantities are defined as the square root of the sum of the variance among the eight individual values plus the square of the average of the uncertainties in the parameter values yielded by the individual fits. The fits to these eight models were then repeated with $\mathfrak{D}_e$ and R_e held fixed at these average values, and an optimum potential chosen on the basis of requirements that it have only a single inflection point, and that the functional behavior of its vibrational spacings and rotational constants be similar to those for the better defined $a\,^3\Sigma^+$-state alkali pairs. The potential selected is the MLR function with $p=3$, $N_S=1$, and $N_L=6$ whose parameters are listed in Table V. The number of digits required to represent the various parameters with no loss of precision in representing the experimental data was minimized using the sequential rounding and refitting procedure of Ref. 35, which is incorporated in program DPOTFIT.[27] No uncertainties are given for the fitted ϕ_i values, since these parameters have no independent physical significance.

For both the observed species $^{39}K^6Li$ and its more abundant, but unobserved isotopologue $^{39}K^7Li$, listings of the vibrational energies and rotational constants of all bound levels calculated from our final recommended potential are included in the on-line supplementary data.[18] A rough near-dissociation theory analysis[15,16] indicates that the extrapolated vibrational quantum number at the intercept is $v_{\mathfrak{D}}\approx13.18$ for $^{39}K^6Li$ and $v_{\mathfrak{D}}\approx14.11$ for $^{39}K^7Li$, and that the highest vibrational level of each isotopologue has no bound rotationally excited sublevels. Their binding energies, 0.0013 cm^{-1} for $v=13$ of $^{39}K^6Li$ and 0.0002 cm^{-1} for $v=14$ of $^{39}K^7Li$, are much smaller than the approximately ±0.005 cm^{-1} uncertainties in the experimental transition energies and the ±0.07 cm^{-1} uncertainty in the ground-state dissociation energy[11] which locates our potential asymptote. However, the noninteger parts of these $v_{\mathfrak{D}}$ values are sufficiently large that it is likely that these very weakly bound levels do exist. Finally, fitting the lowest vibrational energies to polynomials in $(v+1/2)$ yields approximate equilibrium parameters $\omega_e=47.3(\pm1.4)$ and 44.2(±1.5) cm^{-1} for $^{39}K^6Li$ and $^{39}K^7Li$, respectively, where the uncertainty mainly reflects the distribution of values associated with our eight good-fit potentials.

TABLE V. Parameters defining our recommended $MLR_{p=3}$ ($N_S=1$, $N_L=6$) potential function for $a\,^3\Sigma^+$ state KLi. The dimensionless rms deviation for the associated fit to the 147 data was 1.05.

$\mathcal{D}_e$ (cm^{-1})	287.0(±4.0)
R_e (Å)	4.99(±0.09)
C_6 (cm^{-1} Å^6)	1.119×10^7
C_8 (cm^{-1} Å^6)	2.63×10^8
ϕ_0	−2.12675
ϕ_1	0.0554
ϕ_2	20.026
ϕ_3	−144.25
ϕ_4	371.6
ϕ_5	−422.0
ϕ_6	180.0

V. CONCLUSIONS

A striking aspect of the present work is the fact that an analysis based only on information for six vibrational levels lying in the upper third of the potential well yields a well-defined overall potential energy function for the $a\,^3\Sigma^+$ state of KLi. The excellent agreement with the combining-rule predictions seen in Table IV attests both to the reliability of this result and to the fact that the *ab initio* estimate of the well depth is probably ~5% too small. It is also remarkable to see the degree of agreement in the low energy extrapolation region among the independent fitted potentials shown in Fig. 5 for each of the three vibrational assignments considered. This ability to determine a good overall potential from such a limited data set is due to the effectiveness of the direct-potential-fit approach, to the the robustness of the MLR potential function form, and probably partly to the fact that this attractive van der Waals well is bound entirely by inverse-power dispersion energy terms.

The absolute vibrational assignments would have been even more secure had it been possible to observe transitions involving the $a\,^3\Sigma^+$ state of the $^{39}K^7Li$ isotopologue. However, efforts to excite $^{39}K^7Li$ levels close to 19 100 cm^{-1} did not produce triplet emission. The only collisional bands observed for the main isotopologue were finally assigned, not as triplet bands but as transitions from high vibrational levels of the (experimentally unknown) $A\,^1\Sigma^+$ state to $v''=45$ and 46 of the $X\,^1\Sigma^+$ state. The upper triplet state of K^6Li populated by collisional energy transfer is not known, but is assumed to be $c\,^3\Sigma^+$, because of the *R* and *P* branches observed in emission. Franck-Condon factors calculated between our $a\,^3\Sigma^+$ potential and the difference potential between the *ab initio* $a\,^3\Sigma^+$ and $c\,^3\Sigma^+$ potentials suggest it should be possible to observe a small number of consecutive vibrational levels of $a\,^3\Sigma^+$, starting at $v=5$.

The partial picture of the $a\,^3\Sigma^+$ state of KLi yielded by the present high-temperature experiments is analogous to the situation for KRb, for which the photoassociation results of Wang *et al.*[3] only included levels bound by up to 30 cm^{-1}, and the vibrational analysis had to be based on comparisons with *ab initio* results.[36] In the present case, however, we have shown that a well-defined overall potential energy curve could be determined directly from the experimental data. On the other hand, the match between observed intensities and Franck-Condon factor patterns is not entirely satisfactory in either case. In spite of these shortcomings of the data, the present work yields what is believed to be a reliable overall analytical potential energy function which incorporates the correct known long-range behavior, and yields an excellent fit to all the available experimental data. It also provides realistic predictions of the unobserved levels near the potential minimum and asymptote, although the overall estimated uncertainty in T_e is approximately 4 cm^{-1}.

This collaboration was supported by the French-Polish exchange program "Polonium" and by the PAN-CNRS bilateral exchange scheme. Two of the authors (P.K. and W.J.) also acknowledge support from the Polish Ministry of Science and Higher Education (Grant No. N202 103 31/0753). Another author (R.J.L.) is pleased to acknowledge research support from the Natural Sciences and Engineering Research Council of Canada.

[1] C. Haimberger, J. Kleinert, O. Dulieu, and N. P. Bigelow, J. Phys. B **39**, S957 (2006).
[2] S. D. Kraft, P. Staanum, J. Lange, L. Vogel, R. Wester, and M. Weidemüller, J. Phys. B **39**, S993 (2006).
[3] D. Wang, E. E. Eyler, P. L. Gould, and W. C. Stwalley, Phys. Rev. A **72**, 032502 (2005).
[4] H. Wang and W. C. Stwalley, J. Chem. Phys. **108**, 5767 (1998).
[5] A. Altmeyer, S. Riedel, C. Kohstall, M. J. Wright, R. Geursen, M. Bartenstein, C. Chin, J. Hecker Benschlag, and R. Grimm, Phys. Rev. Lett. **98**, 040401 (2007).
[6] W. Jastrzębski, P. Kowalczyk, and A. Pashov, J. Mol. Spectrosc. **209**, 50 (2001).
[7] S. Rousseau, A. R. Allouche, M. Aubert-Frécon, S. Magnier, P. Kowalczyk, and W. Jastrzebski, Chem. Phys. **247**, 193 (1999).
[8] R. Rydberg, Z. Phys. **73**, 376 (1931); O. Klein, *ibid.* **76**, 226 (1932); R. Rydberg, *ibid.* **80**, 514 (1933); A. L. G. Rees, Proc. Phys. Soc. London **59**, 998 (1947).
[9] R. J. Le Roy, Y. Huang, and C. Jary, J. Chem. Phys. **125**, 164310 (2006).
[10] R. J. Le Roy and R. D. E. Henderson, Mol. Phys. **105**, 663 (2007).
[11] H. Salami, Ph.D. thesis, Université Lyon 1, 2007.
[12] A. Derevianko, J. F. Babb, and A. Dalgarno, Phys. Rev. A **63**, 052704 (2001).
[13] S. G. Porsev and A. Derevianko, J. Chem. Phys. **119**, 844 (2003).
[14] V. Bednarska, I. Jackowska, W. Jastrzebski, and P. Kowalczyk, Meas. Sci. Technol. **7**, 1291 (1996).
[15] R. J. Le Roy and W.-H. Lam, Chem. Phys. Lett. **71**, 544 (1980).
[16] R. J. Le Roy, J. Chem. Phys. **101**, 10217 (1994).
[17] F. Martin, P. Crozet, A. J. Ross, M. Aubert-Frécon, P. Kowalczyk, W. Jastrzębski, and A. Pashov, J. Chem. Phys. **115**, 4118 (2001).
[18] See EPAPS Document No. E-JCPSA6-126-008719 for ASCII files containing listings of the data used in the present work and tabulations of the vibrational energies and rotational constants of all bound levels of $^{39}K^6Li$, and $^{39}K^7Li$, generated from out final recommended potential. This document can be reached via a direct link in the online article's HTML reference section or via the EPAPS homepage (http://www.aip.org/pubservs/epaps.html).
[19] J. W. Tromp and R. J. Le Roy, J. Mol. Spectrosc. **109**, 352 (1985).
[20] D. R. T. Appadoo, R. J. Le Roy, P. F. Bernath, S. Gerstenkorn, P. Luc, J. Vergès, J. Sinzelle, J. Chevillard and Y. D'Aignaux, J. Chem. Phys. **104**, 903 (1996).
[21] A. Pashov, W. Jastrzębski, and P. Kowalczyk, Comput. Phys. Commun. **128**, 622 (2000).
[22] A. Pashov, W. Jastrzębski, and P. Kowalczyk, J. Chem. Phys. **113**, 6624 (2000).
[23] H. G. Hedderich, M. Dulick, and P. F. Bernath, J. Chem. Phys. **99**, 8363 (1993).
[24] Y. Huang, M.Sc. thesis, Department of Chemistry, University of Waterloo, 2001.
[25] R. J. Le Roy and Y. Huang, J. Mol. Struct.: THEOCHEM **591**, 175 (2002).
[26] Y. Huang and R. J. Le Roy, J. Chem. Phys. **119**, 7398 (2003); **126**, 169904(E) (2007).
[27] R. J. Le Roy, J. Seto, and Y. Huang, University of Waterloo Chemical Physics Research Report No. CP-662R, 2006 (see http://leroy.uwaterloo.ca/programs/).
[28] G. C. Maitland, M. Rigby, E. B. Smith, and W. A. Wakeham, *Intermolecular Forces: Their Origin and Determination* (Oxford University Press, Oxford, 1981).
[29] C. Linton, F. Martin, A. J. Ross, I. Russier, P. Crozet, A. Yiannopoulou, L. Li, and A. M. Lyyra, J. Mol. Spectrosc. **196**, 20 (1999).
[30] G. Zhao, W. T. Zemke, J. T. Kim, B. Ji, H. Wang, J. T. Bahns, W. C. Stwalley, L. Li, A. M. Lyyra, and C. Amiot, J. Chem. Phys. **105**, 7976 (1996).
[31] K. Ishikawa, N. Mukai, and M. Tanimura, J. Chem. Phys. **101**, 876 (1994).
[32] A. Pashov (private communication).
[33] Y.-C. Wang, M. Kajitani, S. Kasahara, M. Baba, K. Ishikawa, and H. Katô, J. Chem. Phys. **95**, 6229 (1991).
[34] A. Pashov, O. Docenko, M. Tamanis, R. Ferber, H. Knöckel, and E. Tiemann, Phys. Rev. A **72**, 062505 (2005).

[35] R. J. Le Roy, J. Mol. Spectrosc. **191**, 223 (1998).
[36] W. T. Zemke, R. Côté, and W. C. Stwalley, Phys. Rev. A **71**, 062706 (2005).
[37] V. S. Ivanov, V. B. Sovkov, and L. Li, J. Chem. Phys. **118**, 8242 (2003).
[38] L. Li, A. M. Lyyra, W. T. Luh, and W. C. Stwalley, J. Chem. Phys. **93**, 8452 (1990).
[39] S. Magnier, M. Aubert-Frécon, and P. Millié, J. Mol. Spectrosc. **200**, 96 (2000).